Molecular Biology of the Cell
Vol. 17, 3356–3368, August 2006

Association of Bcl-2 with Misfolded Prion Protein Is Linked to the Toxic Potential of Cytosolic PrP

Angelika S. Rambold,* Margit Miesbauer,* Doron Rapaport,† Till Bartke,‡ Michael Baier,§ Konstanze F. Winklhofer,*‖ and Jörg Tatzelt*‖

*Department of Biochemistry, Neurobiochemistry, Ludwig-Maximilians-Universität München, D-80336 München, Germany; †Institut für Physiologische Chemie, Ludwig-Maximilians-Universität München, D-81377 München, Germany; ‡Department of Pathology, University of Cambridge, Cambridge CB2 1QP, United Kingdom; and §Robert-Koch-Institut, D-13353 Berlin, Germany

Submitted January 27, 2006; Revised April 17, 2006; Accepted May 10, 2006
Monitoring Editor: Jonathan Weissman

Protein misfolding is linked to different neurodegenerative disorders like Alzheimer's disease, polyglutamine, and prion diseases. We investigated the cytotoxic effects of aberrant conformers of the prion protein (PrP) and show that toxicity is specifically linked to misfolding of PrP in the cytosolic compartment and involves binding of PrP to the anti-apoptotic protein Bcl-2. PrP targeted to different cellular compartments, including the cytosol, nucleus, and mitochondria, adopted a misfolded and partially proteinase K–resistant conformation. However, only in the cytosol did the accumulation of misfolded PrP induce apoptosis. Apoptotic cell death was also induced by two pathogenic mutants of PrP, which are partially localized in the cytosol. A mechanistic analysis revealed that the toxic potential is linked to an internal domain of PrP (amino acids 115–156) and involves coaggregation of cytosolic PrP with Bcl-2. Increased expression of the chaperones Hsp70 and Hsp40 prevented the formation of PrP/Bcl-2 coaggregates and interfered with PrP-induced apoptosis. Our study reveals a compartment-specific toxicity of PrP misfolding that involves coaggregation of Bcl-2 and indicates a protective role of molecular chaperones.

INTRODUCTION

Prion diseases are a group of transmissible neurodegenerative disorders including Creutzfeldt-Jakob disease (CJD) and Gerstmann-Sträussler-Scheinker syndrome (GSS) in humans, scrapie in sheep and goat, bovine spongiform encephalopathy (BSE) in cattle and chronic wasting disease (CWD) in free-ranging deer. A hallmark of prion diseases is the conversion of the cellular prion protein PrP^{C} into PrP^{Sc}, a misfolded and proteinase K (PK)-resistant isoform, which is the main component of infectious prions (reviewed in Weissmann *et al.,* 1996; Prusiner *et al.,* 1998; Collinge, 2001; Chesebro, 2003; Aguzzi and Polymenidou, 2004).

In the majority of prion diseases neurodegeneration is tightly linked to the propagation of infectious prions. However, transgenic mouse models revealed that misfolding or mistargeting of PrP^{C} can induce neuronal cell death in the absence of infectious prions. Vice versa, propagation of infectious prions was observed without inducing neuronal cell death, but only when PrP^{C} is not expressed in neurons (reviewed in Winklhofer and Tatzelt, 2006). Moreover, neuronal expression of a secreted PrP mutant devoid of the glycosylphosphatidylinositol (GPI) anchor sustains propagation of infectious prions in the absence of clinical symptoms (Chesebro *et al.,* 2005).

This article was published online ahead of print in *MBC in Press* (http://www.molbiolcell.org/cgi/doi/10.1091/mbc.E06–01–0083) on May 17, 2006.

‖ These authors contributed equally to this work.

Address correspondence to: Jörg Tatzelt (Joerg.Tatzelt@med.uni-muenchen.de).

The biogenesis of PrP^{C} is characterized by a series of co- and posttranslational modifications (reviewed in Tatzelt and Winklhofer, 2004). It involves import of the nascent chain into the endoplasmic reticulum (ER) and the attachment of two N-linked core glycans and a GPI anchor. After processing of the glycans into complex structures in the Golgi compartment, PrP^{C} is targeted to the outer leaflet of the plasma membrane.

Several studies indicated that PrP can acquire a neurotoxic potential when its import into the ER is partially or completely compromised. Lingappa and coworkers demonstrated that during import into the ER, PrP can attain two different transmembrane topologies termed ^{Ctm}PrP and ^{Ntm}PrP (Yost *et al.,* 1990). Interestingly, increased synthesis of ^{Ctm}PrP has been shown to coincide with progressive neurodegeneration both in GSS syndrome patients with an A117V mutation and in transgenic mice carrying a triple mutation within the hydrophobic domain (AV3; Hegde *et al.,* 1998; Stewart *et al.,* 2005). A different transgenic mouse model revealed that preventing the import of PrP into the ER leads to the formation of a neurotoxic PrP species. Mice expressing a PrP mutant with a deleted N-terminal ER targeting signal (cytoPrP) acquired severe ataxia due to cerebellar degeneration and gliosis (Ma *et al.,* 2002). Earlier results already indicated that both wild-type PrP and a PrP mutant associated with an inherited prion disease in humans can be found in the cytosol and are subjected to proteasomal degradation (Ma and Lindquist, 2001; Yedidia *et al.,* 2001). Cytotoxic effects of cytoPrP were also observed in some cell culture models (Ma *et al.,* 2002; Rane *et al.,* 2004), whereas in other studies expression of cytoPrP seemed not to interfere with cellular viability (Roucou *et al.,* 2003; Fioriti *et al.,* 2005). Support for a toxic potential of cytosolically localized PrP was also obtained in a yeast model. During posttranslational targeting of

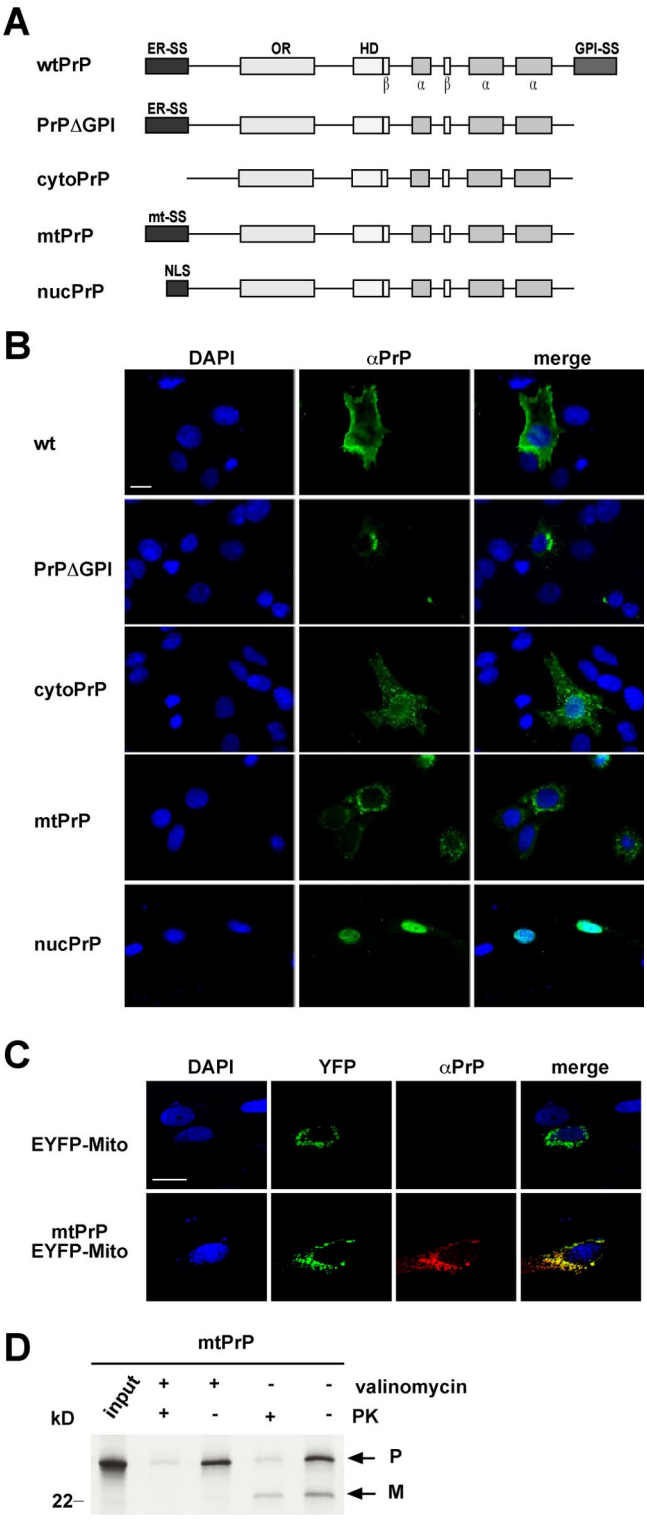

Figure 1. Specific targeting of PrP to different cellular compartments. (A) Schematic presentation of the PrP mutants analyzed. ER-SS, ER signal sequence; OR, octarepeat; HD, hydrophobic domain; α, alpha helix; β, beta strand; GPI-SS, GPI anchor signal sequence; mt-SS, mitochondrial signal sequence; NLS, nuclear localization signal. All mutants are devoid of the GPI-SS (aa 231–253). (B) SH-SY5Y cells were transiently transfected with plasmids encoding wild-type PrP or the mutant prion proteins and analyzed by indirect immunofluorescence using the anti-PrP mAb 3F4 (αPrP). Nuclei were stained with DAPI. (C) Confocal images of SH-SY5Y cells coexpressing mtPrP and EYFP-Mito, which is specifically targeted to mitochondria. Indirect immunofluorescence was performed using the anti-PrP mAb 3F4. (D) mtPrP is imported into mitochondria in vitro. mtPrP cDNA was translated in vitro and the radiolabeled mtPrP (input) was incubated with isolated mitochondria for 20 min at 25°C. To one sample valinomycin was added (valinomycin +) to inhibit mitochondrial import. After import, each sample was divided into two aliquots. From one aliquot the mitochondria were pelleted directly and boiled in sample buffer (PK −). The other aliquot was first treated with PK (500 μg/ml; PK +). All samples were analyzed by SDS-PAGE and autoradiography. P, precursor with the uncleaved mitochondrial targeting signal sequence; M, mature protein. Bars, 15 μm.

PrP to the ER, PrP was missorted to the cytosol and interfered with yeast growth (Heller *et al.*, 2003).

So far, mutations within the N-terminal signal sequence of PrP, which could affect the efficiency of ER import, have not been identified in patients suffering from prion diseases. The analysis of PrP-W145Stop, however, revealed that a pathogenic PrP mutant linked to GSS syndrome, is found in the cytosolic and nuclear compartment (Zanusso *et al.*, 1999). Further studies including a different pathogenic mutant, PrP-Q160Stop, corroborated these findings and revealed that information in the C-terminal domain of PrP is necessary and sufficient for import into the endoplasmic reticulum (Heske *et al.*, 2004).

In this study, we directed PrP to different cellular compartments and analyzed the impact on cell viability. Although in all compartments analyzed PrP adopted a detergent-insoluble, partially PK-resistant conformation, only cytosolic PrP interfered with cell viability and induced apoptosis. The apoptotic potential of cytosolic PrP was linked to an internal domain of PrP, comprising the hydrophobic domain and helix 1, and correlated with the binding of Bcl-2 to misfolded PrP. Binding of Bcl-2 to PrP, as well as apoptosis, could be prevented by the increased expression of Hsp70 and its cochaperone Hsp40, indicating a protective role of chaperones in PrP-induced toxicity.

MATERIALS AND METHODS

Antibodies and Reagents

The following antibodies were used: anti-PrP 3F4 monoclonal antibody (mAb; Kascsak *et al.*, 1987), anti-PrP 3B5 mAb (Krasemann *et al.*, 1996), anti-PrP antiserum A7 (Winklhofer *et al.*, 2003a), anti-ACTIVE caspase-3 polyclonal antibody (pAb; Promega, Madison, WI), anti-Hsp40 pAb (Stressgen, Victoria, British Columbia, Canada), anti-Bcl-2 mouse mAb (BD Biosciences, San Diego, CA), anti-GAPDH mouse mAb (6C5; Calbiochem, La Jolla, CA), Cy3-conjugated anti-mouse IgG antibody and Cy3-conjugated anti-rabbit IgG antibody (Dianova, Hamburg, Germany), anti-FLAG M2 mAb (Sigma, Deisenhofen, Germany), anti-FLAG pAb (rabbit, Sigma), anti-GFP mAb (Roche, Indianapolis, IN). The following reagents were used: MG132 (Calbiochem), PK (Roche), and staurosporin and valinomycin (Sigma). The mounting medium Mowiol (Calbiochem) was supplemented with 4′,6-diamidino-2-phenylindole (DAPI, Sigma).

Plasmids

The following constructs were described previously: wtPrP, PrPΔGPI (Winklhofer *et al.*, 2003c), Q160Stop, W145Stop, cytoPrP (Heske *et al.*, 2004), and EYFP-Hsp70, Hsp40 (Kim *et al.*, 2002; Winklhofer *et al.*, 2003b). All amino acid numbers refer to the mouse PrP sequence (GenBank accession number M18070). For the generation of PrP targeted to the nucleus (nucPrP) or mitochondria (mtPrP), the authentic ER signal sequence of PrP^C was replaced by the nuclear localization signal of SV40 large T antigen (MDPKKKRKV) or the mitochondrial signal sequence of subunit 1 of the ubiquinol cytochrome C reductase complex (MAASAVCRAACSGTQVLLRTRRSPALLRPALRGTATFA), respectively. Human XIAP with a N-terminal FLAG-tag (MDYKDDDDK) was described earlier (Bartke *et al.*, 2004). FLAG-Bcl-2 was generated by fusing a FLAG-tag (DYKDDDDK) to the C-terminus of human Bcl-2 (GenBank accession number AAA51813). As a mitochondrial marker pEYFP-Mito vector (Clontech, Heidelberg, Germany) was used.

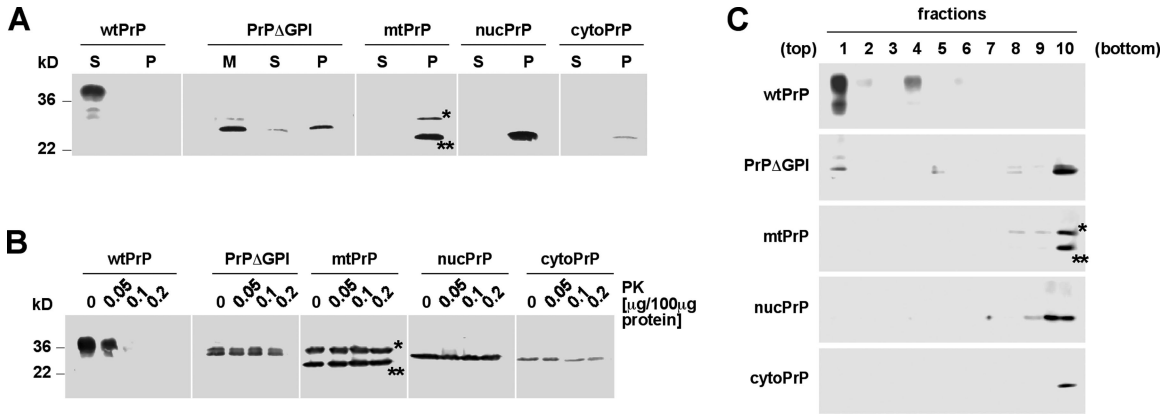

Figure 2. PrP mutants adopt a misfolded and partially PK-resistant conformation. (A–C) SH-SY5Y cells were transiently transfected with wild-type PrP^C or the indicated PrP mutants and analyzed 24 h after transfection. (A) Cells were lysed in cold buffer A and fractionated by centrifugation. PrP present in the detergent-soluble (S) and -insoluble (P) fractions was analyzed by Western blotting using the mAb 3F4. In case of PrPΔGPI, secretion of PrP was analyzed in addition. Cells were cultivated for 3 h in serum-free medium at 37°C, and PrP present in the medium was then analyzed by Western blotting (PrPΔGPI, M). (B) Total cell lysates were treated with increasing concentrations of PK as indicated at 4°C for 30 min. Residual PrP was detected by Western blotting. Molecular size markers are indicated as bars on the left side of the panels. (C) Cells were lysed in gradient buffer (0.5% Triton X-100) and placed on top of a 30–40% sucrose step gradient. After ultracentrifugation 10 fractions were collected from the top of the gradient and analyzed by Western blotting using the anti-PrP antibody 3F4. Precursor and mature form of mtPrP are indicated by * and **, respectively.

Cell Culture, Transfection, Proteasomal Inhibition, and Proteinase K Digestion

SH-SY5Y cells were cultivated as described earlier (Winklhofer *et al.*, 2003c). Cells cultivated on a 3.5-cm cell culture dish (Nunc, Wiesbaden-Biebrich, Germany) were transfected with a total of 2 μg DNA by a liposome-mediated method using LipofectAMINE Plus reagent (Invitrogen, Karlsruhe, Germany) according to the manufacturer's instructions. To keep the amount of transfected cytoPrP constant, a plasmid expressing EYFP or ECFP under the same promoter was added to a total of 2 μg DNA. The proteasomal inhibitor MG132 was dissolved in dimethyl sulfoxide, added to the cell culture medium (30 μM), and incubated for 3 h at 37°C. For proteolysis experiments, cells were lysed in cold buffer A (0.5% Triton X-100, 0.5% sodium deoxycholate [DOC] in phosphate-buffered saline [PBS]) and incubated for 30 min at 4°C with PK at the concentrations indicated. The reaction was terminated by addition of Pefabloc SC (Roche) and boiling in Laemmli sample buffer. Residual PrP was detected by Western blotting.

Detergent Solubility Assay, Western Blotting, and Sucrose Step Gradient

As described earlier (Tatzelt *et al.*, 1996), cells were washed twice with cold saline buffer (PBS), scraped off the plate, pelleted by centrifugation, and lysed in cold buffer A. After centrifugation the detergent-soluble and -insoluble fractions were analyzed by Western blotting. To examine the secretion of PrP into the cell culture supernatant, cells were cultivated in serum-free medium for 3 h at 37°C. Medium was collected, and proteins precipitated with trichloroacetic acid (TCA) and then analyzed by Western blotting. SDS-PAGE and Western blotting were described previously (Winklhofer and Tatzelt, 2000). For sucrose step gradient analysis, cells were lysed in 150 μl gradient buffer containing 0.1% Triton X-100, 25 mM Tris-HCl (pH 7.5), 100 mM NaCl, 5 mM $MgCl_2$, and 5% glycerol. The gradient was performed as described earlier (Henn *et al.*, 2005). Ten fractions were collected from the top of the gradient. The proteins were precipitated by TCA and analyzed by Western blotting.

Scrapie Infection and Preparation of Brain Extracts

Intracerebral infections of C57B/6 mice with scrapie-strain 139A were carried out as previously described (Schultz *et al.*, 2004). Brain extracts were prepared in buffer A (10% w/vol) and fractionated by centrifugation into the detergent-soluble and -insoluble fraction as described above. For PK digestion the whole lysate was adjusted to 1% Sarkosyl and incubated with PK (50 μg/ml) for 1 h at 37°C. The reaction was terminated by addition of Pefabloc SC and boiling in Laemmli sample buffer. Residual PrP was detected by Western blotting using the anti-PrP antiserum A7.

In Vitro Translation and Mitochondrial Import Assay

The in vitro translation was carried out by using the TNT T7 Quick Coupled Transcription/Translation System (Promega) by following the manufacturer's instructions. After translation the samples were used for the mitochondrial import assay as described earlier (Stan *et al.*, 2003). Protein import in yeast mitochondria was performed in SI buffer (3% BSA [w/vol], 0.5 M sorbitol, 50 mM HEPES-KOH, 80 mM KCl, 10 mM MgAc, 2 mM KH_2PO_4, 2.5 mM EDTA, 2.5 mM $MnCl_2$, 2 mM ATP, 2 mM NADH, pH 7.2). Protease treatment of mitochondria was performed by incubation with PK for 15 min on ice, followed by the addition of 1 mM phenylmethylsulfonyl fluoride for 5 min as described before. Products were analyzed by SDS-PAGE. Gels were impregnated with Amplify (GE Healthcare, Waukesha, WI) and exposed to film.

Metabolic Labeling and Immunoprecipitation

Cells were starved for 30 min in methionine-free minimum Eagle's medium (Invitrogen) and subsequently labeled for 45 min with 300 μCi/ml Promix [L-^{35}S] in vitro cell label mix (Amersham Biosciences, Braunschweig, Germany; >37 TBq/mmol) in methionine-free minimum Eagle's medium (pulse). When indicated, the proteasomal inhibitor MG132 was present during starvation, labeling, and chase periods (30 μM final concentration). For the chase, labeling medium was removed, cells were washed twice and then incubated in complete medium for 30 min at 37°C. Immunoprecipitation of PrP was performed as described earlier (Winklhofer *et al.*, 2003c). For the coimmunoprecipitation experiments, low-detergent buffer (0.1% Triton X-100 in PBS) was used for cell lysis and incubation with the antibody. Proteins present in the immunopellet were released by boiling in buffer B (Triton X-100, DOC, Sarkosyl, 0.5% each in PBS) and subjected to a second immunoprecipitation under nonnative conditions.

Co-pullup Experiments

Cells were lysed in low-detergent buffer (0.1% Triton X-100 in PBS) and incubated for 16 h with anti-FLAG M2 mAb at 4°C. To extract FLAG-tagged Bcl-2 proteins, the cell lysate was incubated with magnetic anti-mouse IgG-DYNAbeads (Invitrogen) for 2 h and exposed to a magnetic field for 2 min to pull up bound immunocomplexes. Unbound material was removed and analyzed by Western blotting. After washing, the immunocomplexes were dissolved by boiling in Laemmli sample buffer and analyzed for bound cytoPrP by Western blotting, using the anti-PrP antibody A7. Anti-FLAG M2 mAb was used to detect the Bcl-2 constructs.

Indirect Immunofluorescence and Apoptosis Assay

For indirect immunofluorescence experiments, SH-SY5Y cells were grown on glass coverslips, fixed with 3% PFA for 20 min, and permeabilized with 0.2% Triton X-100 for 10 min at room temperature. The primary antibody was incubated for 45 min at 37°C in PBS containing 1% BSA. After extensive washing with cold PBS, an incubation with the Cy3-conjugated secondary antibody followed at 37°C for 30 min. For detection of apoptosis, cells were fixed and permeabilized as described above. Blocking of the cells was performed with 5% horse serum and 0.1% Tween 20 in PBS for 1 h at room temperature. Cells were then incubated with anti-ACTIVE caspase-3 antibody overnight at 4°C, followed by Cy3-conjugated secondary antibody for 1 h at

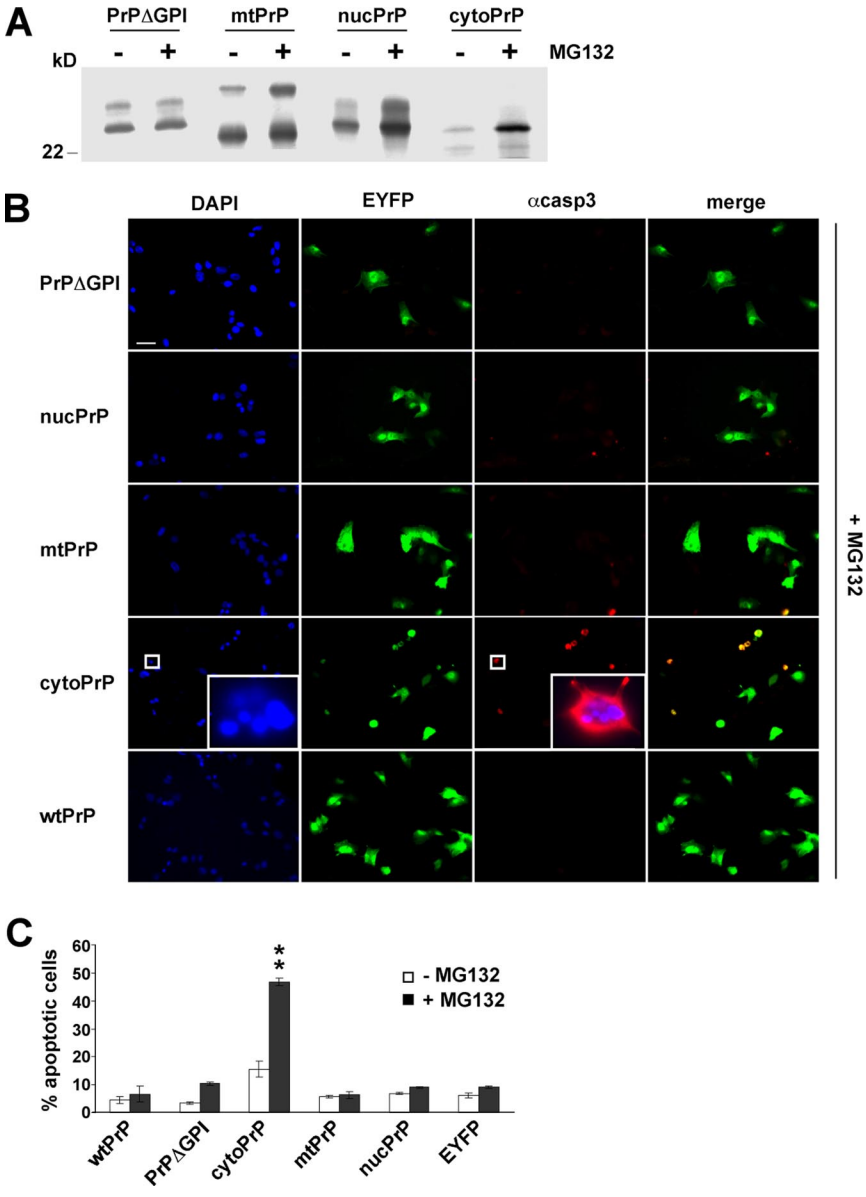

Figure 3. PrP misfolding in the cytosol induces apoptosis. (A) PrP localized in the cytosol and nucleus is degraded by the proteasome. Transiently transfected SH-SY5Y cells were labeled for 45 min with [^{35}S]methionine in the presence (MG132 +) or absence (MG132 −) of the proteasome inhibitor MG132 (30 μM). PrP was then analyzed by immunoprecipitation using the mAb 3F4. (B and C) Cytosolic PrP induces apoptosis after inhibition of the proteasome. SH-SY5Y cells were cotransfected with EYFP and PrP mutants as indicated. Twenty-four hours after transfection cells were incubated with MG132 (30 μM) at 37°C for 3 h, fixed, permeabilized, and analyzed by indirect immunofluorescence. Activation of caspase-3 was detected by using the anti-ACTIVE caspase-3 pAb. Nuclei were stained with DAPI. (C) Quantification of apoptosis. One thousand transfected cells were counted in at least three independent experiments. Shown is the percentage of apoptotic cells among the transfected cells. **p $<$ 0.001 compared with all other PrP mutants and the EYFP control. Bars, 40 μm.

room temperature. Cells were mounted onto glass slides and examined by fluorescence microscopy using a Zeiss Axiovert 200M microscope (Carl Zeiss, Oberkochen, Germany). To analyze the apoptotic potential of the various PrP constructs, the number of activated caspase-3–positive cells out of 1000 transfected cells was determined. All quantifications were based on at least three independent experiments. Confocal images were obtained on a Leica DM IRE2 confocal microscope (Leica, Heidelberg, Germany) and evaluated with the Leica confocal software version 2.6.1.

Statistical Analysis

Data were expressed as means ± SE. All experiments were performed in duplicates and repeated at least three times. Statistical analysis among groups was performed using student's *t* test. P-values are as follows: *p $<$ 0.01, **p $<$ 0.001, and ***p $<$ 0.0001.

RESULTS

PrP Directed to Different Cellular Compartments Adopts a Misfolded Conformation

Previous studies in transgenic mice revealed that misfolding of PrP in the cytosol can induce neurodegeneration (Ma *et al.*, 2002). The neurotoxic PrP conformer present in the cytosol (cytoPrP) is quite distinct from infectious PrP^{Sc}. CytoPrP adopts a misfolded and partially PK-resistant conformation; however, it lacks posttranslational modifications, like the GPI anchor and N-linked carbohydrates; moreover, it does not seem to be infectious. In the present study we addressed the question of whether misfolding of PrP is cytotoxic per se or whether PrP-induced toxicity is linked to the cellular compartment in which PrP adopts a misfolded conformation.

To achieve subcellular targeting of PrP to different compartments, including the nucleus, cytosol, mitochondria and ER, the following constructs were generated: nucPrP with the nuclear localization signal (NLS) of SV40 T antigen, mtPrP with the mitochondrial signal sequence of ubiquinol cytochrome C reductase complex subunit 1, and cytoPrP lacking the authentic ER signal sequence (Figure 1A). To include a PrP conformer that misfolds in the secretory pathway, we used a mutant that contains the N-terminal ER-

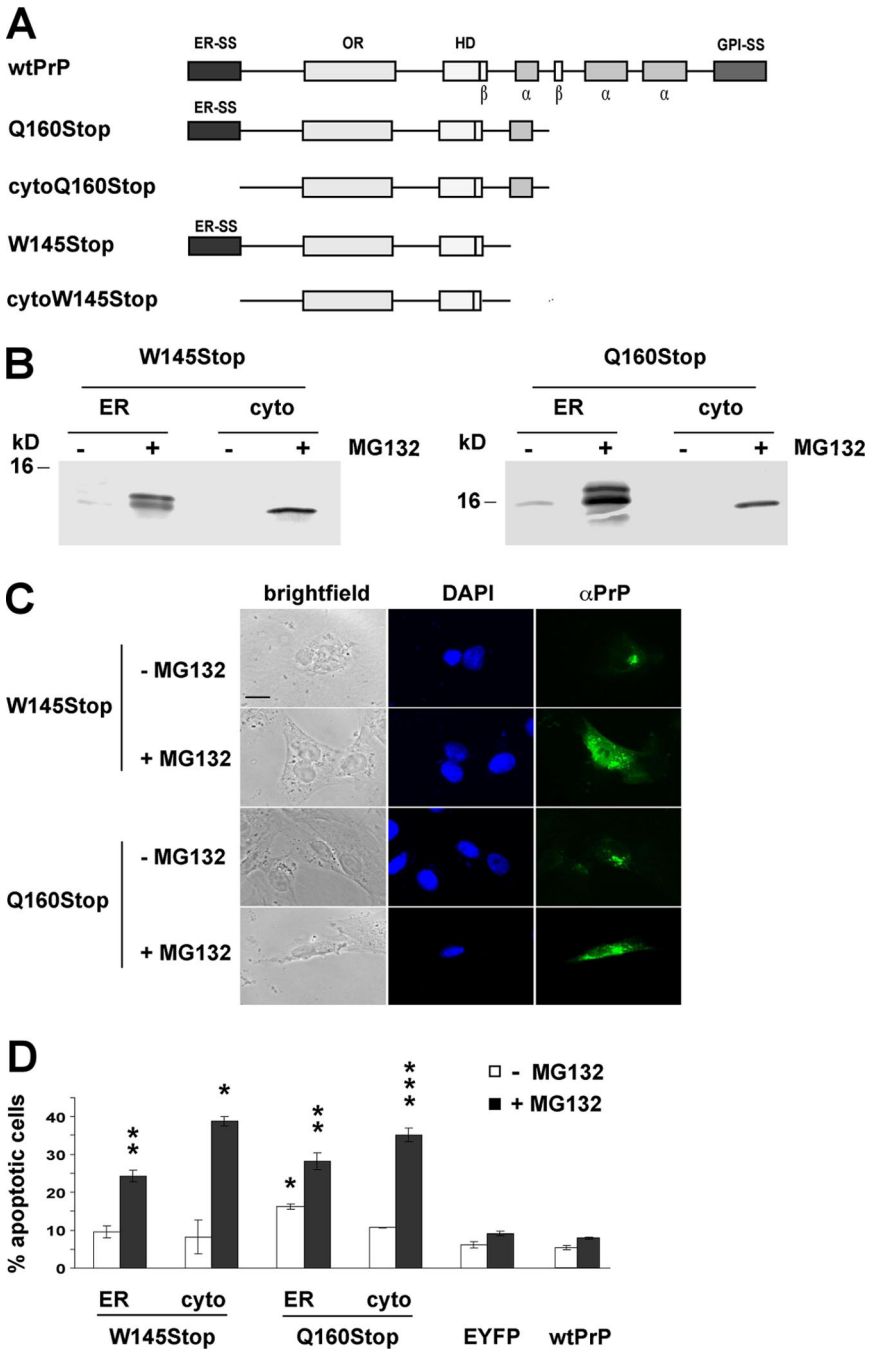

Figure 4. Pathogenic mutants are missorted to the cytosol and induce apoptosis. (A) Schematic presentation of two pathogenic PrP mutants linked to inherited prion diseases in humans. Two versions of each mutant were generated, one version with the authentic N-terminal ER signal sequence (ER-SS) and one for cytosolic expression by deleting the ER-SS (cyto). (B–D) Transiently transfected SH-SY5Y cells expressing the pathogenic mutants either with the ER signal sequence (ER) or without (cyto) were cultivated for 45 min (B) or 3 h (C) in the presence or in the absence of the proteasome inhibitor MG132. PrP was analyzed by immunoprecipitation (B) and indirect immunofluorescence (C) as described in Figure 3. (D) Quantification of apoptosis induced by the pathogenic PrP mutants. Apoptosis was detected by indirect immunofluorescence using the anti-ACTIVE caspase-3 pAb. Shown is the percentage of apoptotic cells among the transfected cells. *$p < 0.01$, **$p < 0.001$, and ***$p < 0.0001$ compared with EYFP-transfected cells. Bars, 15 μm.

targeting signal but lacks the C-terminal GPI signal sequence (designated PrPΔGPI). Targeting to and import into the ER of PrPΔGPI is efficient, but in the secretory pathway PrPΔGPI spontaneously adopts a misfolded conformation and is secreted (Rogers *et al.*, 1993; Blochberger *et al.*, 1997; Winklhofer *et al.*, 2003c).

First, we analyzed the subcellular localization of the different PrP constructs. Indirect immunofluorescence analysis of transiently transfected SH-SY5Y cells revealed that the targeting sequences efficiently directed PrP to the respective cellular compartments (Figure 1B). Targeting of PrP into mitochondria was further confirmed using an in vitro import assay and colocalization analysis (Figure 1, C and D). In addition, import of PrPΔGPI into the ER was corroborated by the detection of secreted PrPΔGPI in the cell culture supernatant (Figure 2A). Notably, SH-SY5Y cells do not express significant levels of endogenous PrP^C (unpublished data). Thus, only the heterologously expressed PrP constructs are detected in our assays.

To compare the conformation of PrP in different cellular compartments, we made use of three biochemical assays: solubility in detergent buffer, sensitivity to a limited PK digestion, and a sedimentation analysis on a sucrose step gradient. In contrast to wild-type PrP^C, all PrP mutants, including PrPΔGPI, were mainly insoluble in detergent buffer (Figure 2A) and showed an increased resistance to proteolytic digestion (Figure 2B). In addition, all mutants formed aggregates. Protein extracts of transiently trans-

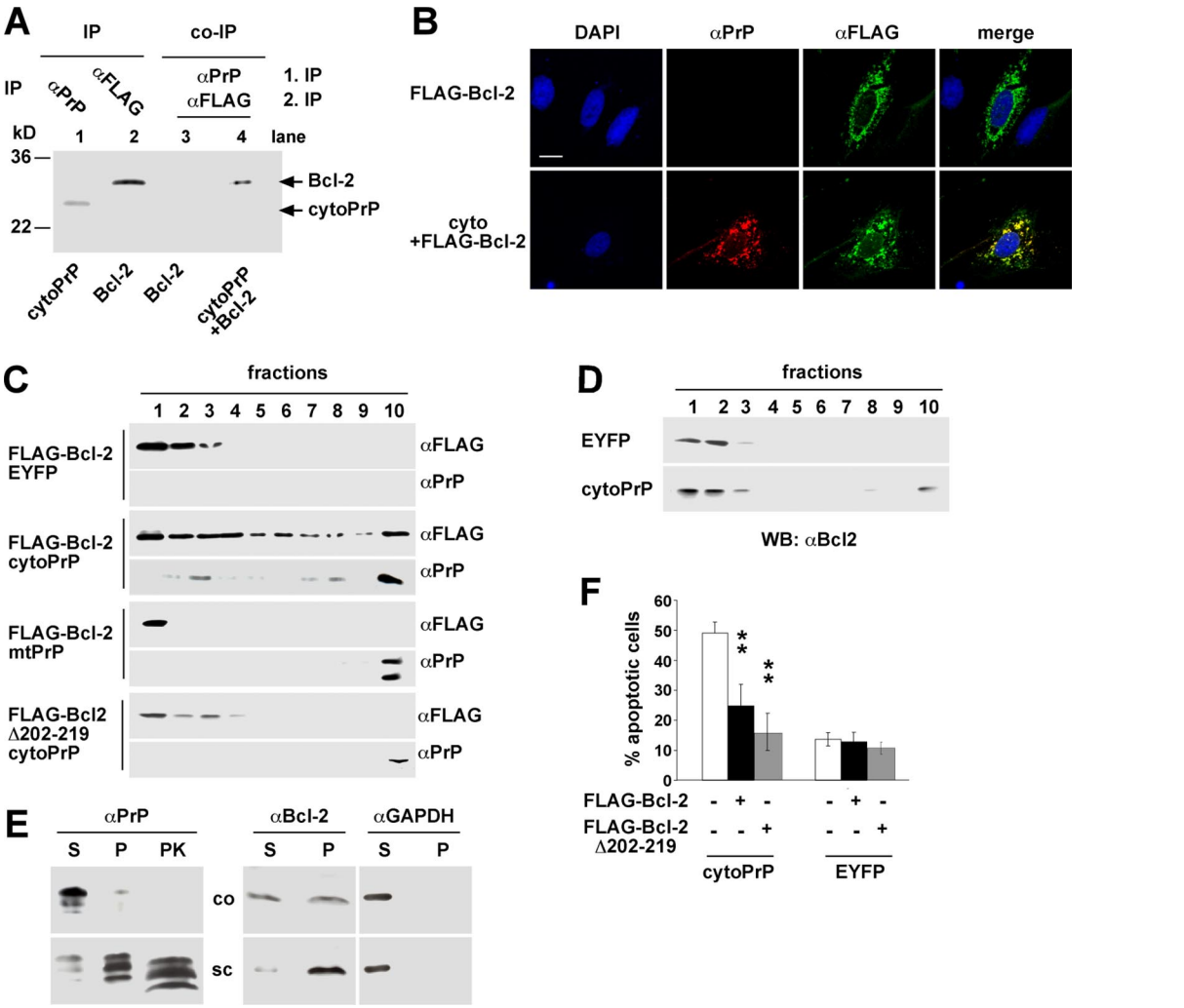

Figure 5. CytoPrP binds to and induces aggregation of Bcl-2. (A and B) CytoPrP interacts with Bcl-2 in SH-SY5Y cells. (A) For coimmunoprecipitation experiments (lanes 3 and 4) SH-SY5Y cells were transfected with cytoPrP and FLAG-tagged Bcl-2 (lane 4) or with Bcl-2 only (lane 3). Cells were metabolically labeled for 45 min in the presence of MG132 (30 μM) and lysed in low-detergent buffer. After immunoprecipitation of PrP under native conditions with the anti-PrP antibody 3B5 (1. IP, αPrP), proteins released from the immunopellet were subjected to a second immunoprecipitation under nonnative conditions using an anti-FLAG antibody (2. IP, αFLAG). As a control, PrP and Bcl-2 were analyzed by immunoprecipitation under nonnative conditions (lanes 1 and 2). (B) Transfected cells were analyzed by indirect immunofluorescence using the anti-FLAG pAb and the PrP-specific 3F4 mAb by confocal microscopy. (C) CytoPrP induces aggregation of Bcl-2 but not of Bcl-2Δ202–219. Cells were cotransfected with FLAG-tagged Bcl-2 or Bcl-2Δ202–219 and either EYFP, cytoPrP, or mtPrP. Total cell lysates were prepared in gradient buffer, loaded on a 30–40% sucrose step gradient, and centrifuged at 200,000 × *g* for 90 min at 4°C. Ten fractions were collected from the top of the gradient, proteins were precipitated by TCA and immunoblotted for FLAG-Bcl-2 and PrP, respectively. A long exposure image was used for FLAG-Bcl-2 + cytoPrP (αPrP) to show that cytoPrP also localizes to the upper fractions of the gradient. (D) CytoPrP interacts with endogenous Bcl-2. SH-SY5Y cells were transfected with either EYFP or cytoPrP. CytoPrP-induced aggregation of endogenous Bcl-2 was analyzed by centrifugation through a 30–40% sucrose step gradient as described in C. (E) Brain extracts of terminally scrapie-ill (sc) and control (co) mice were prepared and fractionated by centrifugation into the detergent-soluble (S) and -insoluble fraction (P). Samples were analyzed by Western blotting for PrP, Bcl-2, and GAPDH, respectively. In addition, one sample was digested with proteinase K to specifically detect PrP^{Sc} (αPrP, PK). (F) Overexpression of Bcl-2 and Bcl-2Δ202–219 interferes with cytoPrP-induced apoptosis. Cells were transfected with cytoPrP alone or cotransfected with cytoPrP and Bcl-2 or Bcl-2Δ202–219. Apoptotic cells were identified by indirect immunofluorescence using the anti-ACTIVE caspase-3 pAb. Shown is the percentage of apoptotic cells among the transfected cells. **$p < 0.001$ compared with cytoPrP-expressing cells. Bars, 15 μm.

fected cells were applied on top of a sucrose step gradient. After centrifugation all mutant PrP constructs were found in the bottom fraction, whereas wild-type PrP^{C} remained in the top fractions (Figure 2C).

These experiments established that PrP can efficiently be targeted to different cellular compartments. The biochemical properties of the PrP mutants present in the nucleus, cytosol, mitochondria and ER are similar and indicate the formation of misfolded and aggregated conformers.

Apoptosis Is Selectively Induced by Misfolding of PrP in the Cytosol

The Western blot analysis indicated that the steady state level of cytoPrP was considerably lower than that of the other PrP mutants (Figure 2A). The most plausible explanation for this phenomenon was proteasomal degradation of cytoPrP. Indeed, after proteasomal inhibition by MG132 (3 h, 30 μM) the relative levels of cytoPrP and

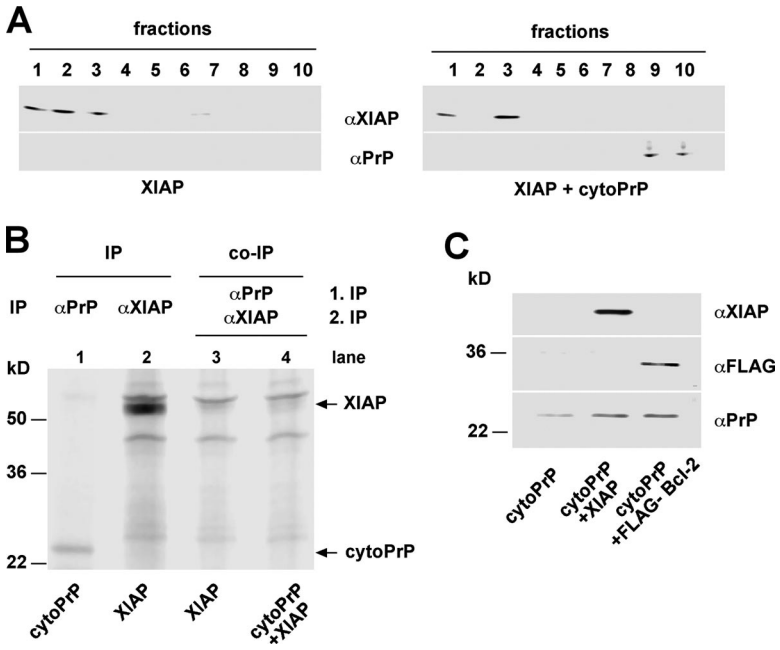

Figure 6. CytoPrP neither interacts with nor induces aggregation of XIAP. (A) CytoPrP does not induce aggregation of XIAP. SH-SY5Y cells were transfected with XIAP and XIAP/cytoPrP, respectively. The sedimentation profile of XIAP and cytoPrP was analyzed by a sucrose step gradient as described in Figure 5. (B) XIAP does not interact with cytoPrP. SH-SY5Y cells expressing XIAP alone or in combination with cytoPrP were analyzed by coimmunoprecipitation experiments as described in Figure 5 (lanes 3 and 4). After a first immunoprecipitation under native conditions using the anti-PrP antibody 3B5, proteins in the immunopellet were analyzed by a second immunoprecipitation under nonnative conditions using an anti-XIAP antibody (lanes 3 and 4). As a control, PrP and XIAP were analyzed by immunoprecipitation under nonnative conditions from cells expressing either PrP or XIAP (lanes 1 and 2). (C) Coexpression of Bcl-2 or XIAP does not interfere with expression of cytoPrP. SH-SY5Y cells were cotransfected with cytoPrP/ECFP, cytoPrP/Bcl-2, or cytoPrP/XIAP. The cells were lysed in cold buffer A and analyzed by immunoblotting using the indicated antibodies.

nucPrP were significantly increased, whereas the proteasome inhibitor had no significant effect on the relative amount of PrP imported into the ER or mitochondria (Figure 3A).

Next, we analyzed possible adverse effects of misfolded PrP on cellular viability. To identify cells undergoing apoptosis, transiently transfected neuroblastoma cells were analyzed by indirect immunofluorescence using an antibody specific for activated caspase-3. The specificity of the antibody was confirmed in control experiments with cells subjected to increasing concentrations of staurosporine, a known inducer of apoptosis. Under physiological culture conditions, expression of cytoPrP slightly increased the number of apoptotic cells, whereas expression of the other PrP mutants did not result in caspase-3 activation above control conditions, i.e., expression of wild-type PrP^C or cytosolic EYFP (Figure 3C, −MG132). The cytotoxic effect of cytoPrP was significantly enhanced in cells transiently exposed to the proteasomal inhibitor MG132. Importantly, transient treatment with MG132 neither induced apoptosis in cells expressing PrP^C or cytosolic EYFP nor in cells harboring misfolded PrP in the mitochondria, the nucleus, or the ER (Figure 3, B and C, +MG132). The enhanced toxicity of cytoPrP in MG132-treated cells correlated with the increased amount of cytoPrP in these cells (Figure 3A, +MG132). However, it is important to note that the increased level of cytoPrP is not sufficient to explain its cytotoxic effect, because the relative amount of cytoPrP never exceeded that of PrPΔGPI, mtPrP, or nucPrP (Figure 3A and unpublished data). In this context it is interesting to note that a small fraction of mtPrP contained an uncleaved signal peptide, but did not induce apoptosis. It is possible that this precursor, although localized in the cytosol, is already associated with the mitochondria import machinery or bound to cytosolic proteins, like Hsp70, which are involved in targeting to and import into mitochondria.

Thus, a toxic potential of misfolded PrP was specifically linked to its cytosolic localization. Cellular viability was not affected by misfolded PrP present in other cellular compartments, be it the ER, the mitochondria, or the nucleus.

Pathogenic Mutations Linked to Inherited Prion Diseases in Humans Are Mistargeted to the Cytosol and Induce Apoptosis

The above experiments demonstrated that mistargeting of PrP to the cytosol can effectively induce apoptosis. The question remained whether such a mistargeting could play a role in the pathogenesis of human prion diseases. Previous studies indicated that upon proteasomal degradation wild-type and mutant D177N PrP accumulates in the cytosol (Ma and Lindquist, 2001; Yedidia *et al.*, 2001). Similarly, we and others showed that Q160Stop and W145Stop (Figure 4A), two pathogenic PrP mutants characterized by large C-terminal deletions, are partially present in the cytosol and are subjected to proteasomal degradation (Zanusso *et al.*, 1999; Heske *et al.*, 2004). This phenomenon is illustrated by an immunoprecipitation analysis of transiently transfected SH-SY5Y cells cultivated for 3 h in the presence of MG132 before the sample preparation (Figure 4B, +MG132). In addition, an indirect immunofluorescence analysis indicated a significant increase of cytosolically localized Q160Stop and W145Stop after transient proteasomal inhibition (Figure 4C). Two scenarios are conceivable to explain this phenomenon. Either the C-terminal deletion mutants are subjected to ER-associated protein degradation (ERAD) or their import into the ER is partially compromised.

Consequently, we tested whether these pathogenic mutants can interfere with cellular viability. Indeed, expression of Q160Stop and W145Stop induced apoptosis similarly to cytoPrP (Figure 4D). To specifically analyze the cytosolic fraction of these mutants, we generated cytosolic versions of these mutants, which lack the N-terminal ER signal sequence and thus are exclusively targeted to the cytosol (Figure 4A). Apoptosis was significantly increased after the expression of cytoQ160Stop and cytoW145Stop, indicating that the cytosolic fractions seem to be responsible for the toxic effects of Q160Stop and W145Stop (Figure 4D).

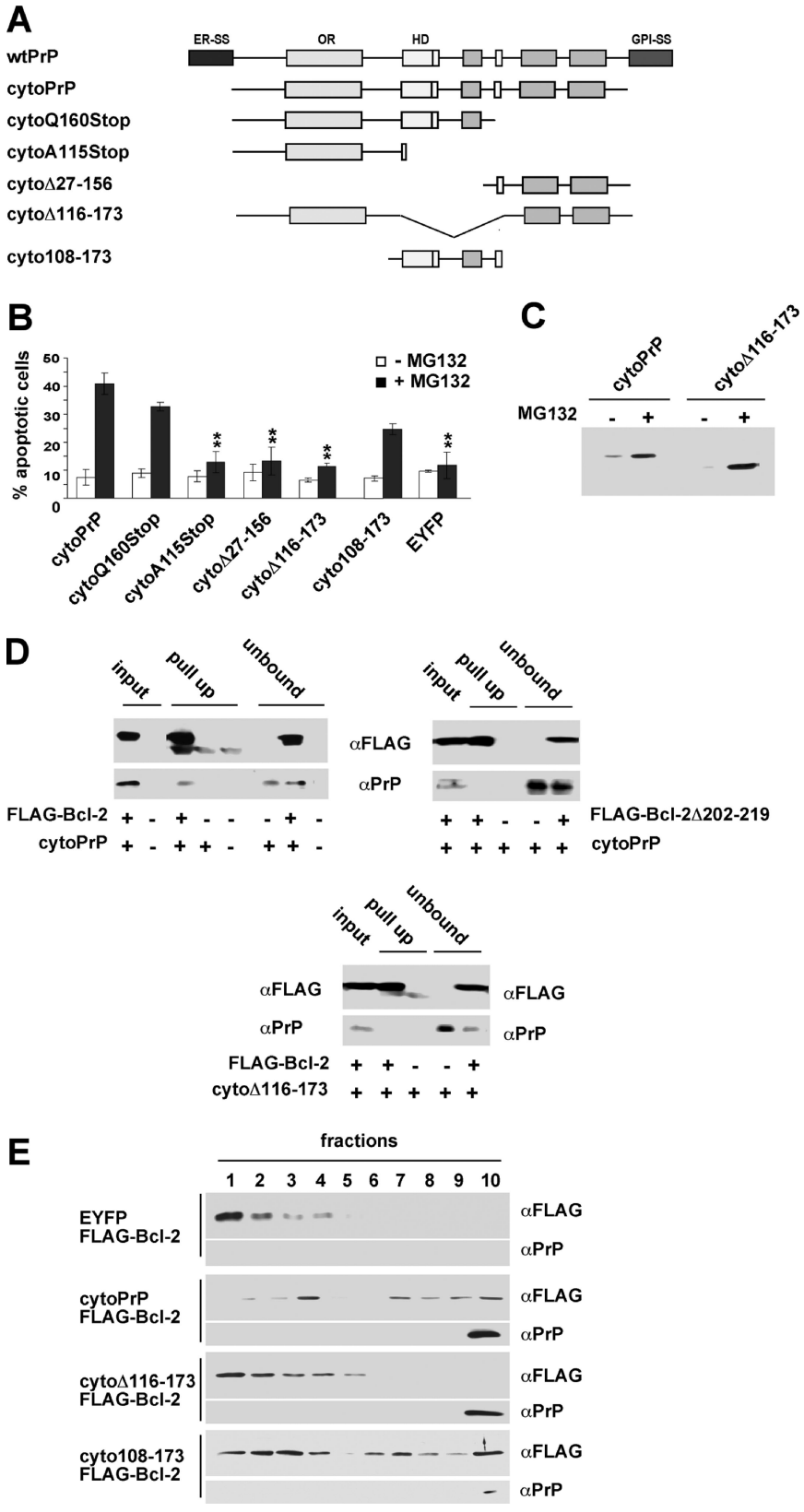

Figure 7. The toxic potential of cytoPrP resides within the proximal part of the C-terminal domain. (A) Schematic representation of cytosolic PrP deletion mutants. (B) SH-SY5Y cells were cotransfected with EYFP and the PrP mutants as indicated. Twenty-four hours after transfection, the cells were cultivated for additional 3 h in the presence or absence of the proteasome inhibitor MG132 (30 μM). Apoptotic cells were identified by indirect immunofluorescence using the anti-ACTIVE caspase-3 pAb. One thousand transfected cells were counted in at least three independent experiments. Shown is the percentage of apoptotic cells among the transfected cells. **$p < 0.001$ compared with cytoPrP-expressing cells. (C) Transiently transfected SH-SY5Y cells expressing the PrP mutants were cultivated 3 h in the presence or absence of the proteasome inhibitor MG132. Cells were lysed in cold buffer A and fractionated by centrifugation. PrP was analyzed by Western blotting using the mAb 3F4. (D) SH-SY5Y cells were transfected with FLAG-Bcl-2/cytoPrP, FLAG-Bcl-2Δ202–219/cytoPrP, and FLAG-Bcl-2/cytoΔ116–173 as indicated. Cells were lysed in low-detergent buffer and incubated with anti-FLAG M2 mAb. The cell lysate was subjected to pull up experiments using magnetic beads coupled with anti-mouse IgG. Bound immunocomplexes (pull up) and unbound material (unbound) were analyzed for cytoPrP by immunoblotting using the 3F4 mAb. (E) Cells were cotransfected with FLAG-tagged Bcl-2 and PrP constructs as indicated. Total cell lysates were prepared in gradient buffer, loaded on a 30–40% sucrose step gradient, and centrifuged at 200,000 × g for 90 min at 4°C. Ten fractions were collected from the top of the gradient, proteins were precipitated by TCA, and immunoblotted for FLAG-Bcl-2 and PrP.

These findings revealed that two pathogenic PrP mutants, linked to inherited prion diseases in humans, are missorted to the cytosol and induce apoptosis. In addition, these experiments indicated that the distal region of the globular C-terminal domain (aa 146–231) is dispensable for the toxic effect of cytosolic PrP.

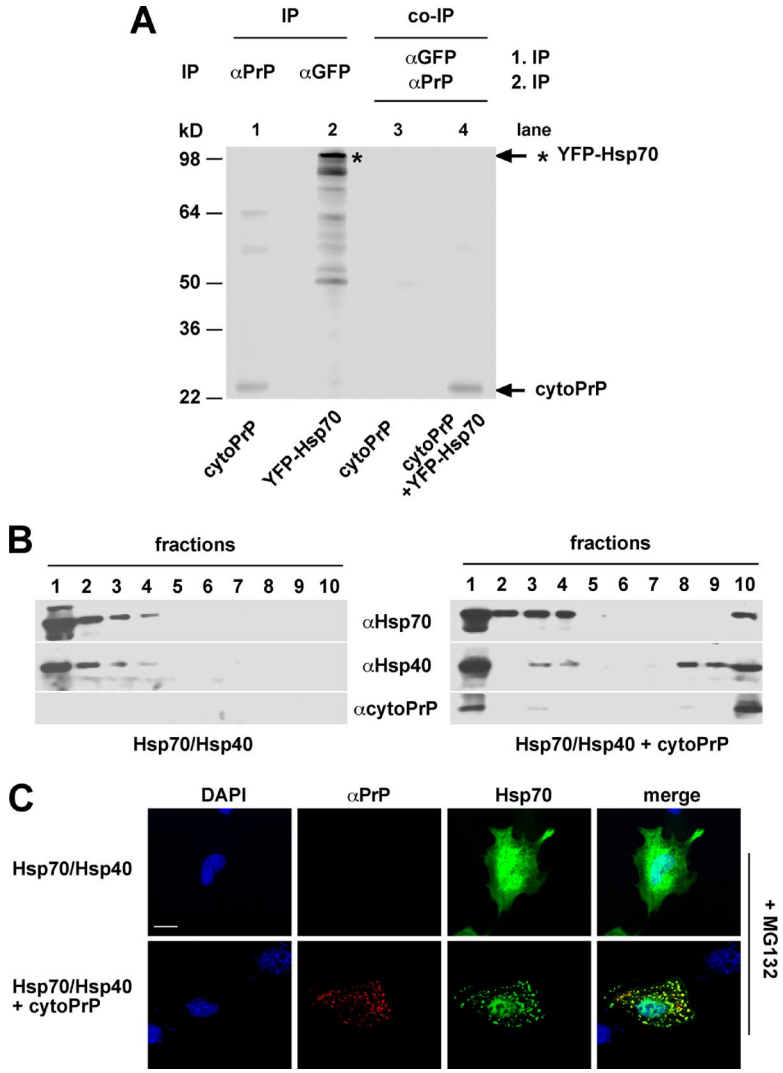

Figure 8. Cytosolic chaperones interact with cytoPrP. (A) The cytosolic chaperone Hsp70 interacts with cytoPrP in SH-SY5Y cells. For coimmunoprecipitations, SH-SY5Y cells were cotransfected with cytoPrP and YFP-Hsp70 (lane 4) or with cytoPrP only (lane 3). Cells were metabolically labeled for 45 min in the presence of MG132 (30 μM) and lysed in low-detergent buffer. After an immunoprecipitation of YFP-Hsp70 under native conditions with the anti-GFP antibody (1. IP, αGFP) proteins in the immunopellet were subjected to a second immunoprecipitation under nonnative conditions using the anti-PrP mAb 3F4 (2. IP, αPrP). As a control, expression of PrP and YFP-Hsp70 was analyzed by immunoprecipitation under nonnative conditions (lanes 1 and 2). (B and C) The cytosolic chaperones Hsp70 and Hsp40 coaggregate with cytoPrP. Cells were cotransfected with YFP-Hsp70/Hsp40 or YFP-Hsp70/Hsp40/cytoPrP. (B) Total cell lysates were prepared in gradient buffer, loaded on a 30–40% sucrose step gradient and centrifuged at 200,000 $\times$ *g* for 90 min at 4°C. Ten fractions were collected from the top of the gradient, proteins were precipitated by TCA and immunoblotted for YFP-Hsp70, Hsp40, and PrP, respectively. (C) Confocal images of SH-SY5Y cells coexpressing Hsp70/Hsp40 and cytoPrP. Indirect immunofluorescence was performed using the anti-PrP mAb 3F4. YFP-Hsp70 is shown in green, and nuclei are stained with DAPI. Bars, 15 μm.

Cytosolic PrP Binds to and Coaggregates with Bcl-2

Previous in vitro studies showed that PrP can interact with the anti-apoptotic protein Bcl-2 and mapped the interaction site to the carboxy terminus of Bcl-2 (aa 200–236; Kurschner and Morgan, 1995, 1996). Consequently, we tested whether an interaction of cytosolic PrP with Bcl-2 occurs in our cell culture model. First, we analyzed a possible interaction of PrP with Bcl-2 by coimmunoprecipitation experiments. Transiently transfected cells expressing both cytoPrP and FLAG-tagged Bcl-2 were metabolically labeled with [^{35}S]methionine. The cells were then lysed in low-detergent buffer, and PrP was immunoprecipitated with the mAb 3B5 under native conditions. Proteins bound to the immunopellet were subsequently released by boiling in detergent buffer B, and a second immunoprecipitation was performed using the anti-FLAG antibody to isolate FLAG-tagged Bcl-2. Bcl-2 copurified under these conditions, indicating that cytoPrP interacts with Bcl-2 in neuronal cells (Figure 5A, lane 4). Importantly, the same procedure did not purify Bcl-2 from cells that do not express cytoPrP (Figure 5A, lane 3) or from cells expressing wtPrP (unpublished data). Moreover, Bcl-2Δ202–219, a mutant with a deletion in the PrP-interacting domain (Kurschner and Morgan, 1996), did not interact with cytoPrP either (see Figure 7D). In addition, we demonstrated colocalization of cytoPrP with Bcl-2 in intact cells by indirect immunofluorescence (Figure 5B).

To analyze whether the interaction of Bcl-2 with PrP has an impact on the biochemical properties of Bcl-2, cells were cotransfected with FLAG-tagged Bcl-2 and either EYFP or cytoPrP or mtPrP. Protein extracts were prepared in gradient buffer and layered on top of a sucrose step gradient. After centrifugation 10 fractions were collected and analyzed by Western blotting. In the absence of cytoPrP, Bcl-2 remained in the top fractions (Figure 5C, EYFP). In cells coexpressing cytoPrP, however, Bcl-2 cosedimented with cytoPrP and was also found in the bottom fraction (Figure 5C, cytoPrP). Notably, no sedimentation of Bcl-2 was observed in the presence of mitochondrial PrP (Figure 5C, mtPrP). Similarly, FLAG-Bcl-2Δ202–219 was not recruited into cytoPrP aggregates (Figure 5C, FLAG-Bcl-2Δ202–219). Coaggregation was not restricted to overexpressed FLAG-Bcl-2 as cytoPrP also induced aggregation of endogenous Bcl-2 (Figure 5D). In this context it is important to note that the cells coexpressing Bcl-2 and cytoPrP were vital and did not undergo apoptosis, due to the overexpression of Bcl-2.

Assuming that the aggregation of Bcl-2 could be of pathophysiological relevance to prion diseases, we analyzed Bcl-2 in brain extracts prepared from terminally scrapie-ill mice.

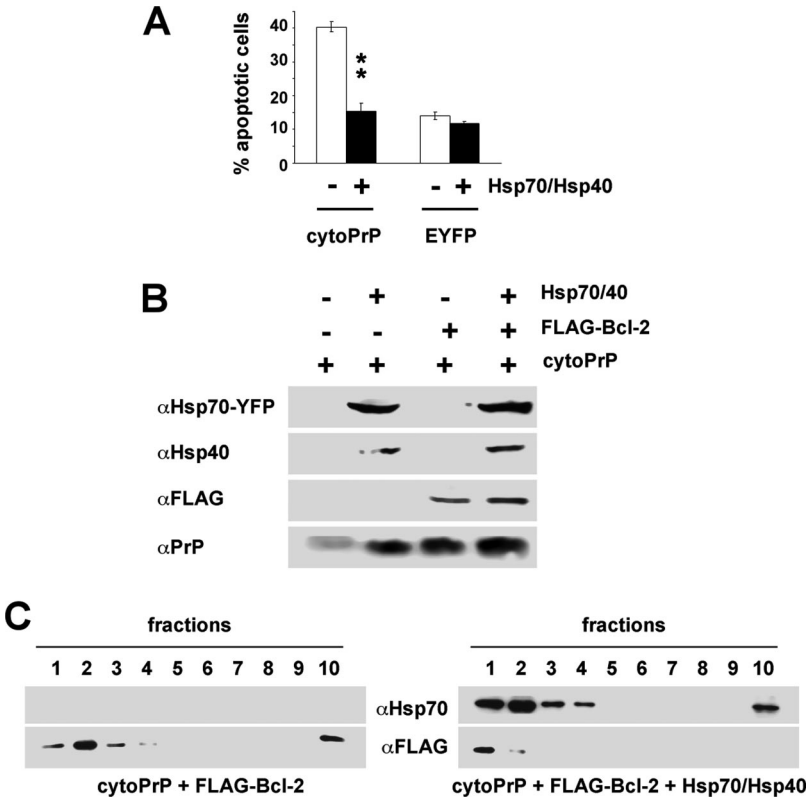

Figure 9. Cytosolic chaperones interfere with cyto-PrP-induced apoptosis and aggregation of Bcl-2. (A) Overexpression of Hsp70 and Hsp40 interferes with PrP-induced apoptosis. SH-SY5Y cells were transfected as indicated and treated with MG132 (30 μM) for 3 h. Apoptotic cells were identified by indirect immunofluorescence using the anti-ACTIVE caspase-3 pAb. The percentage of apoptotic cells among the transfected cells is shown. **$p < 0.001$ compared with cytoPrP-expressing cells. (B) Coexpression of Bcl-2 or Hsp70/40/Bcl-2 does not interfere with the expression of cytoPrP. To keep the amount of transfected cytoPrP constant, a plasmid expressing EYFP under the same promoter was added to a total of 2 μg DNA. Cells were lysed in cold buffer A and analyzed by immunoblotting using the indicated antibodies. (C) Overexpression of Hsp70 and Hsp40 interferes with PrP-induced aggregation of Bcl-2. SH-SY5Y cells were transiently cotransfected with cytoPrP/Bcl-2 and cytoPrP/Bcl-2/YFP-Hsp70/Hsp40, respectively. Whole cell lysates were analyzed on a 30–40% sucrose step gradient. Fractions were collected and immunoblotted against YFP-Hsp70 and FLAG-Bcl-2.

In contrast to the uninfected control, Bcl-2 was predominantly detergent-insoluble in the scrapie-diseased brain (Figure 5E, sc). Of note, infection of the brain with scrapie-prions did not cause protein aggregation in general. Glyceraldehyde-3-phosphate dehydrogenase (GAPDH), a cytosolic protein, was found in the detergent-soluble fraction in both the control and scrapie-infected brain samples (Figure 5E).

If the interaction of PrP with Bcl-2 correlates with the toxic potential of cytoPrP, coexpression of Bcl-2 should alleviate the apoptotic effects of cytoPrP. To test this possibility, apoptosis was analyzed in cells expressing both Bcl-2 and cytoPrP. Indeed, the coexpression of both Bcl-2 and Bcl-2Δ202–219 interfered with cytoPrP-induced apoptosis (Figure 5F).

In response to apoptotic signals, the release of mitochondrial factors such as cytochrome c leads to the activation of caspase-9 and further on to that of caspase-3. XIAP, a known inhibitor of caspase-9 and -3, suppressed cytoPrP-induced apoptosis when overexpressed in cultured cells. Nonetheless, cytoPrP neither interacted with XIAP in coimmunoprecipitation experiments, nor did it induce the aggregation of XIAP (Figure 6, A and B). This further indicates that cytoPrP does not randomly coaggregate with anti-apoptotic proteins. Notably, the relative levels of cytoPrP were not decreased by the coexpression of Bcl-2 or XIAP (Figure 6C).

The Toxic Potential of cytoPrP Resides within the Proximal Part of the Globular Domain, including the Hydrophobic Domain and Helix 1

To investigate whether the cytotoxic potential of cytoPrP is linked to a specific domain, we created several deletion mutants of cytoPrP (Figure 7A). Interestingly, all mutants devoid of the proximal part of the C-terminal globular domain (aa 116–156), comprising the hydrophobic domain and helix 1, did not induce apoptosis. Furthermore, expression of the internal domain, cyto108–173, induced apoptosis, although less efficiently than cytoPrP (Figure 7B). Importantly, differences in the apoptotic potential of the PrP mutants were not due to differences in the expression levels, because the relative amount of the nontoxic mutant cytoΔ116–173 was comparable to that of cytoPrP (Figure 7C). To provide experimental evidence for a direct association of aggregated Bcl-2 with misfolded PrP, pullup experiments were performed. In this approach Bcl-2 was immunopurified similarly to coimmunoprecipitation described above; however, to avoid centrifugation, magnetic anti-mouse IgG-DYNAbeads were used. The immunocomplexes were pulled up by a magnetic field and analyzed by Western blotting. Again, cyto-PrP copurified under these conditions. However, neither was the nontoxic mutant cytoΔ116–173 pulled up by Bcl-2 nor was cytoPrP bound by Bcl2Δ202–219 (Figure 7D). Further support for the assumption that the formation of Bcl-2/cytoPrP aggregates is linked to apoptosis would be provided if the expression of the nontoxic mutant cytoΔ116–173 does not lead to the aggregation of Bcl-2. Indeed, the sucrose gradient analysis revealed that in contrast to cytoPrP or cyto108–173, cytoΔ116–173 did not induce aggregation of Bcl-2. Notably, the internal deletion did not restore folding of cytoΔ116–173 because the mutant was still found in the bottom fractions of the sucrose gradient (Figure 7E).

Cytosolic Chaperones Bind to cytoPrP and Interfere with PrP-induced Apoptosis and the Formation of PrP/Bcl-2 Coaggregates

The biochemical analysis of cytoPrP revealed a nonnative, misfolded conformation that should be recognized by molecular chaperones. Indeed, in an earlier study indirect immunofluorescence experiments revealed colocalization of

cytoPrP with Hsp70 (Ma and Lindquist, 2001). We therefore analyzed a possible interaction of cytoPrP with the cytosolic chaperones Hsp70 and Hsp40. For coimmunoprecipitation experiments we expressed cytoPrP together with YFP-Hsp70 and Hsp40. Previous experiments established that the chaperone activity of Hsp70 is not compromised by the YFP tag (Kim *et al.,* 2002). After a first immunoprecipitation with an anti-GFP antibody under native conditions, the immunopellet was boiled in detergent buffer B and PrP was immunoprecipitated with the monoclonal anti-PrP antibody 3F4. PrP copurified under these conditions, but only in the presence of Hsp70 (Figure 8A, lane 4). A sucrose step gradient provided further evidence that cytoPrP is bound by the cytosolic chaperones Hsp70 and Hsp40. In the absence of cytoPrP, Hsp70 as well as Hsp40 were exclusively found in the top fractions. When cytoPrP was coexpressed, the chaperones were found in the bottom fraction together with cytoPrP (Figure 8B). Interestingly, the chaperones obviously affected the biochemical properties of cytoPrP. In cells overexpressing Hsp70 and Hsp40, a portion of cytoPrP was found in the top fraction of the sucrose gradient (Figure 8B, compare to Figure 2C). Finally, we performed an indirect immunofluorescence analysis to visualize colocalization of cytoPrP and EYFP-Hsp70 (Figure 8C).

In a next step we wanted to determine whether the interaction of cytoPrP with Hsp70 and Hsp40 modulates the cytotoxic potential of cytoPrP. Indeed, the caspase-3 assay revealed that the coexpression of Hsp70 and Hsp40 interfered with cytoPrP-induced apoptosis. In the presence of Hsp70 and Hsp40 the number of apoptotic cells were reduced to background levels (Figure 9A). Importantly, the relative amount of cytoPrP was not reduced by the coexpression of Hsp70 and Hsp40 (Figure 9B).

As shown above, Bcl-2 binds to and coaggregates with cytoPrP (Figure 5). To test the possibility that coexpression of chaperones modulates this interaction, we biochemically analyzed Bcl-2 in cells expressing Hsp70 and Hsp40 in addition to cytoPrP. As expected, Bcl-2 aggregation was observed in cells expressing cytoPrP; however, coexpression of Hsp70 and Hsp40 interfered with cytoPrP-induced aggregation of Bcl-2 (Figure 9C).

In summary, these results indicate that misfolded cytoPrP is recognized and bound by Hsp70 and Hsp40. As a consequence, the cytotoxic potential of cytoPrP and the formation of PrP/Bcl2 coaggregates are reduced.

DISCUSSION

In this study, we analyzed the biochemical properties and cytotoxic potential of PrP targeted to different cellular compartments. Although PrP adopted a misfolded conformation in all compartments analyzed, i.e., the cytosol, nucleus, ER, and mitochondria, apoptosis only occurred when misfolded PrP accumulated in the cytosol. Our study also revealed that the toxic potential of cytosolic PrP (cytoPrP) correlated with its binding to Bcl-2, which is an essential component of the intracellular apoptotic signaling pathways (Danial and Korsmeyer, 2004).

Biogenesis of PrP^C is characterized by a series of co- and posttranslational modifications (reviewed in Tatzelt and Winklhofer, 2004). Among those, addition of the GPI anchor seems to be of particular importance. Initial experiments in cell culture revealed that a mutant devoid of the C-terminal GPI anchor signal sequence (PrPΔGPI) is imported into the ER but remains mainly unglycosylated, spontaneously adopts a misfolded conformation and is efficiently secreted (Rogers *et al.,* 1993; Blochberger *et al.,* 1997; Winklhofer *et al.,* 2003c). The phenotype of anchorless PrP described in cultured cells was recently confirmed in transgenic mice. Notably, expression of PrPΔGPI did not result in clinical symptoms, at least not during the life span of mice (Chesebro *et al.,* 2005). Biochemically, PrPΔGPI (named GPI(−)PrPsen in the mouse study) is similar to the PrP mutant targeted to the cytosol (cytoPrP): both mutants lack the C-terminal signal sequence, are unglycosylated, and adopt a misfolded conformation. However, transgenic mice expressing cytoPrP acquired severe ataxia with cerebellar degeneration (Ma *et al.,* 2002). Our cell culture model recapitulates the observations in transgenic mice: cytoPrP efficiently induced apoptosis, whereas expression of PrPΔGPI had no obvious effect on cellular viability. How can the obvious difference in the neurotoxic potential of PrPΔGPI and cytoPrP be explained? Possibly, the neurotoxic potential is linked to a specific conformation, and the conformation of PrPΔGPI and cytoPrP may be different. Alternatively, the cellular compartment in which PrP misfolding occurs is crucial. Our study provides experimental evidence that the cellular compartment might play a significant role. PrP mutants targeted to the cytosol, nucleus, ER, or mitochondria showed similar biochemical features, yet apoptosis was exclusively induced by cytosolic PrP.

Although the pathophysiological role of cytoPrP might be restricted to a subset of prion diseases, there are several ways to generate of cytoPrP in vivo. It was recently shown that the signal sequence of PrP is insufficient for complete protein translocation into the ER, giving rise to a nontranslocated PrP fraction in the cytosol (Rane *et al.,* 2004). In line with these results, the pathogenic mutants Q160Stop and W145Stop are partially mislocalized in the cytosol (Zanusso *et al.,* 1999; Heske *et al.,* 2004), and we could show that the toxic potential is indeed linked to the cytosolic fraction of these mutants. Alternatively, access to the cytosol is possible via retrograde translocation of PrP out of the ER; this route has been demonstrated for wild-type PrP and another pathogenic PrP mutant, D177N (Ma and Lindquist, 2001; Yedidia *et al.,* 2001). Finally, the generation of transmembrane forms of PrP, which is favored by some pathogenic mutations, leads to the partial exposure of PrP to the cytosol (reviewed in Hegde *et al.,* 1999). Notably, a quantitative study of the ultrastructural localization of PrP in mouse brain revealed that PrP is present in the cytosol in subpopulations of neurons (Mironov *et al.,* 2003).

What might be the mechanism underlying the toxic potential of cytoPrP? Recruitment of anti-apoptotic Bcl-2 to misfolded PrP provides a plausible explanation for the observed effects. An interaction of PrP and Bcl-2 was described previously for recombinantly expressed proteins (Kurschner and Morgan, 1995, 1996). We now show for the first time that such an interaction can occur in neuronal cells and seems to be of pathophysiological relevance. First, only PrP mutants with a toxic potential induced aggregation of Bcl-2. Bcl-2 did not aggregate in cells expressing mitochondrially localized PrP or the nontoxic cytosolic PrP mutant cytoPrPΔ116–173. Second, overexpression of Bcl-2 interfered with cytotoxicity induced by cytoPrP. Third, Bcl-2Δ202–219, a functionally active mutant with a deletion in the PrP-interacting domain, did not coaggregate with cytoPrP, but did interfere with cytoPrP-induced apoptosis. Fourth, the protective effect of Hsp70/Hsp40 in cytoPrP-induced toxicity correlated with their potential to interfere with the recruitment of Bcl-2 into cytoPrP aggregates. Finally, Bcl-2 adopted a detergent-insoluble conformation in scrapie-diseased mouse brain. This interesting observation might provide a link between prion propagation and intracellular apoptotic signaling pathways.

Support for the possibility that PrP^{Sc} itself could induce apoptosis through caspase activation was provided previously in a cell culture model (Hetz *et al.*, 2003). In addition, aggresome formation in scrapie-infected cells was shown to induce caspase-3 activation and apoptosis (Kristiansen *et al.*, 2005). In this context it is also interesting to note that an interaction of PrP with NRAGE, another protein involved in neuronal apoptosis, was reported recently (Bragason and Palsdottir, 2005).

The exact mechanism by which Bcl-2 exerts its anti-apoptotic function is not fully understood, but binding to pro-apoptotic members of the Bcl-2 family seems to be crucial. Regarding the role of Bcl-2 in cytoPrP-mediated toxicity, two scenarios are conceivable. Bcl-2 may be inactivated by its sequestration into cytoPrP aggregates. In support of this possibility, a recent study revealed that aggregation of Bcl-2 can be of pathophysiological relevance for another neurodegenerative disease. It was shown that the amyotrophic lateral sclerosis (ALS)-associated SOD1 mutant proteins bind to and aggregate with Bcl-2 (Pasinelli *et al.*, 2004). Alternatively, binding of Bcl-2 to cytoPrP may induce a conformational change of Bcl-2, converting it to a proapoptotic protein. Evidence for opposing phenotypes of Bcl-2 was provided by Lin *et al.* (2004), who showed that the interaction with Nurr77 converts Bcl-2 from a protector to a killer protein.

Our study clearly revealed that PrP-induced toxicity can be modulated by various cellular factors. Obviously, proteasomal degradation and chaperone activity have a major impact on the formation of toxic PrP conformers. To disclose the cytotoxic potential of cytoPrP, it was necessary to transiently inhibit the proteasome. In untreated cells cytoPrP was hardly detectable by Western blotting, suggesting that the main effect of MG132 was to elevate the amount of cytoPrP. However, it is also conceivable that cells stressed by proteasomal impairment are sensitized to cytoPrP. Similarly, the relative level of Bcl-2 determines whether or not apoptosis is induced by cytoPrP. Efficiency of the ubiquitin-proteasome system as well as chaperone activity decrease with aging, supporting the notion that aged neurons are particularly vulnerable to the accumulation of misfolded proteins. In this context, inefficiencies in the signal-sequence–mediated translocation of PrP into the ER might further promote the generation and accumulation of cytosollically localized PrP conformers. This multifaceted influence on the formation and clearance of cytoPrP, which is highly dependent on the cellular homeostasis, also provides a plausible explanation for the discrepancy between different reports on the toxic potential of cytosolic PrP (Ma *et al.*, 2002; Roucou *et al.*, 2003; Rane *et al.*, 2004; Fioriti *et al.*, 2005).

ACKNOWLEDGMENTS

We thank F. Ulrich Hartl for his support. We are grateful to Richard I. Morimoto for the EYFP-Hsp70 plasmid and to William J. Welch for the Hsp40 plasmid. We also thank Shrukry J. Habib for experimental help with the mitochondrial import assays; Christian Pohl, Christian Schuberth, and Stefan Hümmer for helpful discussions; and Lindsay A. Smale for critical reading the manuscript. This work was supported by grants from the Deutsche Forschungsgemeinschaft (WI 2111/1 and SFB 596), from the Bayerische Staatsminister für Wissenschaft, Forschung, und Kunst (forPrion, MPI3), and from the Max-Planck-Society.

REFERENCES

Aguzzi, A., and Polymenidou, M. (2004). Mammalian prion biology: one century of evolving concepts. Cell *116*, 313–327.

Bartke, T., Pohl, C., Pyrowolakis, G., and Jentsch, S. (2004). Dual role of BRUCE as an antiapoptotic IAP and a chimeric E2/E3 ubiquitin ligase. Mol. Cell *14*, 801–811.

Blochberger, T. C., Cooper, C., Peretz, D., Tatzelt, J., Griffith, O. H., Baldwin, M. A., and Prusiner, S. B. (1997). Prion protein expression in Chinese hamster ovary cells using a glutamine synthetase selection and amplification system. Protein Eng. *10*, 1465–1473.

Bragason, B. T., and Palsdottir, A. (2005). Interaction of PrP with NRAGE, a protein involved in neuronal apoptosis. Mol. Cell. Neurosci. *29*, 232–244.

Chesebro, B. (2003). Introduction to the transmissible spongiform encephalopathies or prion diseases. Br. Med. Bull. *66*, 1–20.

Chesebro, B. *et al.* (2005). Anchorless prion protein results in infectious amyloid disease without clinical scrapie. Science *308*, 1435–1439.

Collinge, J. (2001). Prion diseases of humans and animals: their causes and molecular basis. Annu. Rev. Neurosci. *24*, 519–550.

Danial, N. N., and Korsmeyer, S. J. (2004). Cell death: critical control points. Cell *116*, 205–219.

Fioriti, L., Dossena, S., Stewart, L. R., Stewart, R. S., Harris, D. A., Forloni, G., and Chiesa, R. (2005). Cytosolic prion protein (PrP) is not toxic in N2a cells and primary neurons expressing pathogenic PrP mutations. J. Biol. Chem. *280*, 11320–11328.

Hegde, R. S., Mastrianni, J. A., Scott, M. R., DeFea, K. A., Tremblay, P., Torchia, M., DeArmond, S. J., Prusiner, S. B., and Lingappa, V. R. (1998). A transmembrane form of the prion protein in neurodegenerative disease. Science *279*, 827–834.

Hegde, R. S., Tremblay, P., Groth, D., DeArmond, S. J., Prusiner, S. B., and Lingappa, V. R. (1999). Transmissible and genetic prion diseases share a common pathway of neurodegeneration [see comments]. Nature *402*, 822–826.

Heller, U., Winklhofer, K. F., Heske, J., Reintjes, A., and Tatzelt, J. (2003). Post-translational import of the prion protein into the endoplasmic reticulum interferes with cell viability: a critical role for the putative transmembrane domain. J. Biol. Chem. *278*, 36139–36147.

Henn, I. H., Gostner, J. M., Tatzelt, J., and Winklhofer, K. F. (2005). Pathogenic mutations inactivate parkin by distinct mechanisms. J. Neurochem. *92*, 114–122.

Heske, J., Heller, U., Winklhofer, K. F., and Tatzelt, J. (2004). The C-terminal domain of the prion protein is necessary and sufficient for import into the endoplasmic reticulum. J. Biol. Chem. *279*, 5435–5443.

Hetz, C., Russelakis-Carneiro, M., Maundrell, K., Castilla, J., and Soto, C. (2003). Caspase-12 and endoplasmic reticulum stress mediate neurotoxicity of pathological prion protein. EMBO J. *22*, 5435–5445.

Kascsak, R. J., Rubenstein, R., Merz, P. A., Tonna-DeMasi, M., Fersko, R., Carp, R. I., Wisniewski, H. M., and Diringer, H. (1987). Mouse polyclonal and mAb to scrapie-associated fibril proteins. J. Virol. *61*, 3688–3693.

Kim, S., Nollen, E. A., Kitagawa, K., Bindokas, V. P., and Morimoto, R. I. (2002). Polyglutamine protein aggregates are dynamic. Nat. Cell. Biol. *4*, 826–831.

Krasemann, S., Groschup, M. H., Harmeyer, S., Hunsmann, G., and Bodemer, W. (1996). Generation of monoclonal antibodies against human prion proteins in PrP0/0 mice. Mol. Med. *2*, 725–734.

Kristiansen, M., Messenger, M. J., Klohn, P.C., Brandner, S., Wadsworth, J. D., Collinge, J., and Tabrizi, S. J. (2005). Disease-related prion protein forms aggresomes in neuronal cells leading to caspase-activation and apoptosis. J. Biol. Chem. Sep 12; *Epub ahead of print*.

Kurschner, C., and Morgan, J. I. (1995). The cellular prion protein (PrP) selectively binds to Bcl-2 in the yeast two-hybrid system. Brain Res. Mol. Brain Res. *30*, 165–168.

Kurschner, C., and Morgan, J. I. (1996). Analysis of interaction sites in homo- and heteromeric complexes containing Bcl-2 family members and the cellular prion protein. Brain Res. Mol. Brain Res. *37*, 249–258.

Lin, B., Kolluri, S. K., Lin, F., Liu, W., Han, Y. H., Cao, X., Dawson, M. I., Reed, J. C., and Zhang, X. K. (2004). Conversion of Bcl-2 from protector to killer by interaction with nuclear orphan receptor Nur77/TR3. Cell *116*, 527–540.

Ma, J., and Lindquist, S. (2001). Wild-type PrP and a mutant associated with prion disease are subject to retrograde transport and proteasome degradation. Proc. Natl. Acad. Sci. USA *98*, 14955–14960.

Ma, J., Wollmann, R., and Lindquist, S. (2002). Neurotoxicity and neurodegeneration when PrP accumulates in the cytosol. Science *298*, 1781–1785.

Mironov, A. J., Latawiec, D., Wille, H., Bouzamondo-Bernstein, E., Legname, G., Williamson, R. A., Burton, D., DeArmond, S. J., Prusiner, S. B., and Peters, P. J. (2003). Cytosolic prion protein in neurons. J. Neurosci. *23*, 7183–7193.

Pasinelli, P., Belford, M. E., Lennon, N., Bacskai, B. J., Hyman, B. T., Trott, I. D., and Brown, R. H. (2004). Amyotrophic lateral sclerosis-associated SOD1

mutant proteins bind and aggregate with Bcl-2 in spinal cord mitochondria. Neuron *43*, 19–30.

Prusiner, S. B., Scott, M. R., DeArmond, S. J., and Cohen, F. E. (1998). Prion protein biology. Cell *93*, 337–348.

Rane, N. S., Yonkovich, J. L., and Hegde, R. S. (2004). Protection from cytosolic prion protein toxicity by modulation of protein translocation. EMBO J. *23*, 4550–4559.

Rogers, M., Yehiely, F., Scott, M., and Prusiner, S. B. (1993). Conversion of truncated and elongated prion proteins into the scrapie isoform in cultured cells. Proc. Natl. Acad. Sci. USA *90*, 3182–3186.

Roucou, X., Guo, Q., Zhang, Y., Goodyer, C. G., and LeBlanc, A. C. (2003). Cytosolic prion protein is not toxic and protects against Bax-mediated cell death in human primary neurons. J. Biol. Chem. *278*, 40877–40881.

Schultz, J., Schwarz, A., Neidhold, S., Burwinkel, M., Riemer, C., Simon, D., Kopf, M., Otto, M., and Baier, M. (2004). Role of interleukin-1 in prion disease-associated astrocyte activation. Am. J. Pathol. *165*, 671–678.

Stan, T., Brix, J., Schneider-Mergener, J., Pfanner, N., Neupert, W., and Rapaport, D. (2003). Mitochondrial protein import: recognition of internal import signals of BCS1 by the TOM complex. Mol. Biol. Cell. *23*, 2239–2250.

Stewart, R. S., Piccardo, P., Ghetti, B., and Harris, D. A. (2005). Neurodegenerative illness in transgenic mice expressing a transmembrane form of the prion protein. J. Neurosci. *25*, 3469–3477.

Tatzelt, J., Prusiner, S. B., and Welch, W. J. (1996). Chemical chaperones interfere with the formation of scrapie prion protein. EMBO J. *15*, 6363–6373.

Tatzelt, J., and Winklhofer, K. F. (2004). Folding and misfolding of the prion protein in the secretory pathway. Amyloid *11*, 162–172.

Weissmann, C., Fischer, M., Raeber, A., Büeler, H., Sailer, A., Shmerling, D., Rülicke, T., Brandner, S., and Aguzzi, A. (1996). The role of PrP in pathogenesis of experimental scrapie. Cold Spring Harb. Symp. Quant. Biol. *61*, 511–522.

Winklhofer, K. F., Heller, U., Reintjes, A., and Tatzelt, J. (2003a). Inhibition of complex glycosylation increases formation of PrPSc. Traffic *4*, 313–322.

Winklhofer, K. F., Henn, I. H., Kay-Jackson, P., Heller, U., and Tatzelt, J. (2003b). Inactivation of parkin by oxidative stress and C-terminal truncations; a protective role of molecular chaperones. J. Biol. Chem. *278*, 47199–47208.

Winklhofer, K. F., Heske, J., Heller, U., Reintjes, A., Muranji, W., Moarefi, I., and Tatzelt, J. (2003c). Determinants of the in vivo-folding of the prion protein: a bipartite function of helix 1 in folding and aggregation. J. Biol. Chem. *278*, 14961–14970.

Winklhofer, K. F., and Tatzelt, J. (2000). Cationic lipopolyamines induce degradation of PrPSc in scrapie-infected mouse neuroblastoma cells. Biol. Chem. *381*, 463–469.

Winklhofer, K. F., and Tatzelt, J. (2006). The role of chaperones in Parkinson's disease and prion diseases. In: Molecular Chaperones in Health and Diseases, Vol. 172, ed. M. Gaestel, New York: Springer-Verlag, 221–258.

Yedidia, Y., Horonchik, L., Tzaban, S., Yanai, A., and Taraboulos, A. (2001). Proteasomes and ubiquitin are involved in the turnover of the wild-type prion protein. EMBO J. *20*, 5383–5391.

Yost, C. S., Lopez, C. D., Prusiner, S. B., Myers, R. M., and Lingappa, V. R. (1990). Non-hydrophobic extracytoplasmic determinant of stop transfer in the prion protein. Nature *343*, 669–672.

Zanusso, G., Petersen, R. B., Jin, T., Jing, Y., Kanoush, R., Ferrari, S., Gambetti, P., and Singh, N. (1999). Proteasomal degradation and N-terminal protease resistance of the codon 145 mutant prion protein. J. Biol. Chem. *274*, 23396–23404.